Article

Fluorescence Correlation Spectroscopy, a Tool to Investigate Supramolecular Dynamics: Inclusion Complexes of Pyronines with Cyclodextrin

Wajih Al-Soufi, Beln Reija, Mercedes Novo, Suren Felekyan, Ralf Khnemuth, and Claus A. M. Seidel

J. Am. Chem. Soc., **2005**, 127 (24), 8775-8784• DOI: 10.1021/ja0508976 • Publication Date (Web): 27 May 2005

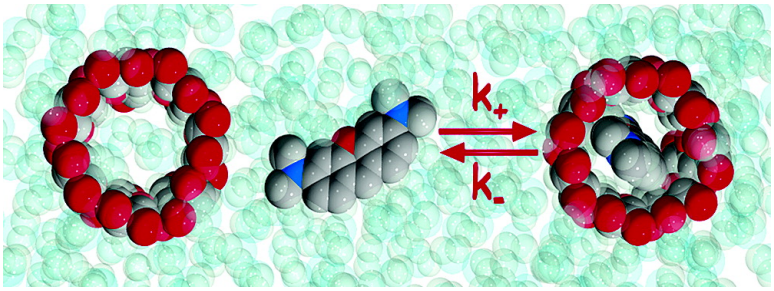

More About This Article

Additional resources and features associated with this article are available within the HTML version:

- Supporting Information
- Links to the 4 articles that cite this article, as of the time of this article download
- Access to high resolution figures
- Links to articles and content related to this article
- Copyright permission to reproduce figures and/or text from this article

View the Full Text HTML

J|A|C|S
ARTICLES
Published on Web 05/27/2005

Fluorescence Correlation Spectroscopy, a Tool to Investigate Supramolecular Dynamics: Inclusion Complexes of Pyronines with Cyclodextrin

Wajih Al-Soufi,*,† Belén Reija,† Mercedes Novo,† Suren Felekyan,‡ Ralf Kühnemuth,‡ and Claus A. M. Seidel‡

Contribution from the Departamento de Química Física, Facultade de Ciencias, Universidade de Santiago de Compostela, E-27002 Lugo, Spain, and Lehrstuhl für Molekulare Physikalische Chemie, Heinrich-Heine Universität Düsseldorf, Universitätsstrasse 1, D-40225 Düsseldorf, Germany

Received February 11, 2005; E-mail: alsoufi@lugo.usc.es

Abstract: The control of supramolecular systems requires a thorough understanding of their dynamics on a molecular level. We present fluorescence correlation spectroscopy (FCS) as a powerful spectroscopic tool to study supramolecular dynamics with single molecule sensitivity. The formation of a supramolecular complex between β-cyclodextrin (β-CD) as host and pyronines Y (PY) and B (PB) as guests is studied by FCS. Global target analysis of full correlation curves with a newly derived theoretical model yields in a single experiment the fluorescence lifetimes and the diffusion coefficients of free and complexed guests and the rate constants describing the complexation dynamics. These data give insight into the recently published surprising fact that the association equilibrium constant of β-CD with PY is much lower than that with the much bulkier guest PB. FCS shows that the stability of the complexes is dictated by the dissociation and not by the association process. The association rate constants are very similar for both guests and among the highest reported for this type of systems, although much lower than the diffusion-controlled collision rate constant. A two-step model including the formation of an encounter complex allows one to identify the unimolecular inclusion reaction as the rate-limiting step. Simulations indicate that this step may be controlled by geometrical and orientational requirements. These depend on critical molecular dimensions which are only weakly affected by the different alkyl substituents of PY and PB. Diffusion coefficients of PY and PB, of their complexes, and of rhodamine 110 are given and compared to those of similar molecules.

Introduction

Understanding supramolecular dynamics is fundamental for the design and control of functional supramolecular systems.[1−3] Information on the dynamics complements thermodynamic and structural studies, but cannot be derived from these. On the contrary, substrates of similar association equilibrium constants can present very different association/dissociation rate constants.[4] Measuring these typically fast processes is challenging and needs fast kinetic techniques. In this contribution, we evaluate the use of fluorescence correlation spectroscopy (FCS) as a direct spectroscopic method to study supramolecular dynamics with single molecule sensitivity. We study the complexation dynamics between a cyclodextrin (CD) as host and two distinct pyronines as guests (Figure 1) since these constitute a basic supramolecular system with unexpected thermodynamical properties.[5] The analysis of this system by FCS leads to a detailed description of the individual kinetic steps involved.

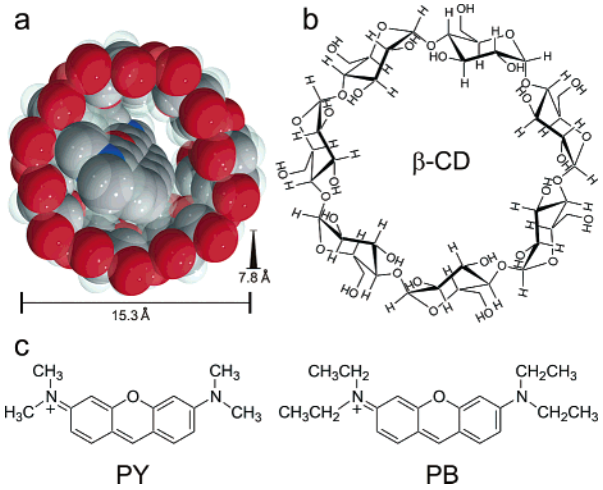

Figure 1. (a) Schematic representation of an inclusion complex between β-CD and PY. (b) Structure of β-CD. (c) Structures of the pyronines PY and PB.

† Universidade de Santiago de Compostela.
‡ Heinrich-Heine Universität Düsseldorf.

(1) Lehn, J. M. *Supramolecular Chemistry*; VCH: Weinheim, Germany, 1995.
(2) Bohne, C. *Spectrum* **2000**, *13* (3), 14−19.
(3) Dyck, A. S. M.; Kisiel, U.; Bohne, C. *J. Phys. Chem. B* **2003**, *107* (42), 11652−11659.
(4) Cramer, F.; Saenger, W.; Spatz, H.-C. *J. Am. Chem. Soc.* **1967**, *89* (1), 14−20.
(5) Reija, B.; Al-Soufi, W.; Novo, M.; Vázquez Tato, J. *J. Phys. Chem. B* **2005**, *109* (4), 1364−1370.

Cyclodextrins are naturally occurring water-soluble toroidally shaped polysaccharides with a highly hydrophobic central cavity that have the ability to form inclusion complexes with a variety of organic and inorganic substrates.[6] The three major cyclodextrins are the α-, β-, and γ-CDs built up from 6, 7, and 8 glucopyranose units, respectively. CDs are often found as building blocks of supramolecular systems and in self-assemblies.[1,7−9] The inclusion complexes result from specific noncovalent interactions between CDs and guest molecules, being therefore also simplified models for the study of molecular recognition phenomena of great importance in host−ligand binding in biological systems.[10,11] Moreover, the ability of CDs to form inclusion complexes, in which the physicochemical properties of the guest molecules change with respect to the free molecules, has led to their widespread industrial use and to applications in green chemistry.[6,12−17]

Whereas the thermodynamic and structural properties of CD complexes have been extensively studied,[5,18−21] the complexation dynamics have been addressed in much less extent.[2,4,22−25] The dynamics of complex association and dissociation, however, not only is of fundamental interest for a better mechanistic understanding of the complexation process itself, a task by far not reached yet, but also is the key to comprehend and to control the huge variety of functions that CDs have to fulfill in the fields mentioned before.

The association equilibrium constant of complexation of organic molecules was found to vary in a wide range from below 10 to several 1000 M^{-1}. The origin of the different complexation constants can only be unraveled using time-resolved spectroscopies which measure the individual steps of complex association and dissociation.

Rate constants of *association* between CDs and different dye molecules were found to vary dramatically from 1 to 10^8 M^{-1} s^{-1} and those of the *dissociation* between 10 to $>10^5$ s^{-1}.[2,4] For the study of rather slow dynamics, stopped-flow experiments were used by some authors.[3,22,23] Fast complexation dynamics between small guest molecules and CDs needs kinetic techniques with high time resolution; Cramer et al. used temperature jump measurements to determine directly the rate constants of both the association and the dissociation process of a series of azo dyes and α-CD. The values correspond to the electronic ground state. They proposed a six-step mechanism for the inclusion complex formation and pointed out the importance of the breakdown and the reconstitution of the water structure around the guest molecule.[4] However, the fast temperature jump required by this technique in order to shift the system away from equilibrium puts a limit to the time resolution and complicates the analysis.[26] Other techniques use long-lived intermediate states populated after light absorption in order to follow equilibrium relaxation; Bohne et al. measured directly the kinetics of complex formation between β-CD and xanthene in its long-lived excited triplet state. In this case, the complexation equilibrium constants of ground and excited triplet states are different, so that the relaxation of the equilibrium can be followed directly after excitation.[2,24] Nau et al. showed that the very long fluorescence lifetime (≈730 ns) of 2,3-diazabicyclo-[2.2.2]oct-2-en is quenched by complexation with β-CD. This can be used to determine the association (but not the dissociation) rate constant of the complexation of the excited singlet state of this compound with β-CD.[25] The above methods yield precise values for the rate constants but are limited to the very special cases presented. The triplet quenching methodology also presented by Bohne et al. is a more general approach to probe excited-state dynamics, but it is necessary to add a quencher molecule to the aqueous phase.[2,24]

The need for external disturbances, quencher molecules, or long-lived intermediate states can be overcome by FCS. FCS is a fluctuation correlation method that measures the dynamics of molecular processes from small changes in molecular concentration or chemical states which arise from spontaneous fluctuations around equilibrium.[27−30] FCS offers in a single measurement an extremely wide dynamic range. Recently, the combination of deadtime-free time-resolved single photon detection with fast software correlation algorithms offers the basis to register full correlation curves from picoseconds to seconds.[31] The use of laser excitation in a confocal setup allows one to work with very small sample volumes and extends the measurement of dynamic processes down to single molecules. FCS has seen a very rapid development in the last years, mainly for biochemical applications, both at the molecular and at the cellular level.[32−35] The feasibility of FCS for monitoring fast biochemical kinetic processes had been shown by Widengren et al.[36] Single molecule multiparameter fluorescence detection (MFD) involves the simultaneous and independent acquisition of several fluorescence parameters (intensity, lifetime, anisotropy

(6) Szejtli, J. *Chem. Rev.* **1998**, *98* (5), 1743−1754.
(7) Harada, A.; Li, J.; Kamachi, M. *Nature* **1993**, *364*, 516.
(8) Nepogodiev, S. A.; Stoddart, J. F. *Chem. Rev.* **1998**, *98* (5), 1959−1976.
(9) Álvarez-Parrilla, E.; Ramos Cabrer, P.; Al-Soufi, W.; Meijide, F.; Rodríguez Núñez, E.; Vázquez Tato, J. *Angew. Chem., Int. Ed.* **2000**, *39* (16), 2856−2858.
(10) Szejtli, J.; Osa, T.; Atwood, J. L. *Comprehensive Supramolecular Chemistry*; Pergamon: Oxford, 1996; Vol. 3.
(11) Breslow, R. *J. Chem. Educ.* **1998**, *75* (6), 705−717.
(12) Loftsson, T.; Brewster, M. E. *J. Pharm. Sci.* **1996**, *85* (10), 1017−1025.
(13) Kaneto Uekama, F. H.; Irie, T. *Chem. Rev.* **1998**, *98* (5), 2045−2076.
(14) Hirayama, F.; Uekama, K. *Adv. Drug Delivery Rev.* **1999**, *36* (1), 125−141.
(15) Breslow, R.; Belvedere, S.; Gershell, L.; Leung, D. *Pure Appl. Chem.* **2000**, *72* (3), 333−342.
(16) Lezcano, M.; Al-Soufi, W.; Novo, M.; Rodríguez Núñez, E.; Vázquez Tato, J. *J. Agric. Food Chem.* **2002**, *50* (1), 108−112.
(17) Ritter, H.; Tabatabai, M. *Prog. Polym. Sci.* **2002**, *27*, 1713−1720.
(18) Connors, K. A. In *Cyclodextrins*; Szejtly, J., Osa, T., Eds.; Elsevier Science: Oxford, 1996; Vol. 3, pp 205−241.
(19) Rekharsky, M. V.; Inoue, Y. *Chem. Rev.* **1998**, *98* (5), 1875−1918.
(20) Fielding, L. *Tetrahedron* **2000**, *56* (34), 6151−6170.
(21) Al-Soufi, W.; Ramos Cabrer, P.; Jover, A.; Budal, R. M.; Vázquez Tato, J. *Steroids* **2003**, *68* (1), 43−53.
(22) Yoshida, N.; Seiyama, A.; Fujimoto, M. *J. Phys. Chem.* **1990**, *94*, 4246.
(23) Yoshida, N.; Hayashi, K. *J. Chem. Soc., Perkin Trans. 2* **1994**, *6*, 1285−1290.
(24) Kleinman, M. H.; Bohne, C. In *Organic Photochemistry*; Ramamurthy, V., Schanze, K., Eds.; Marcel Dekker Inc.: New York, 1997; Vol. 1; pp 391−466.
(25) Zhang, X.; Gramlich, G.; Wang, X.; Nau, W. M. *J. Am. Chem. Soc.* **2002**, *124* (2), 254−263.
(26) Ballew, R. M.; Sabelko, J.; Reiner, C.; Gruebele, M. *Rev. Sci. Instrum.* **1996**, *67* (10), 3694−3699.
(27) Thompson, N. L. In *Topics in Fluorescence Spectroscopy: Techniques*; Lakowicz, J. R., Ed.; Plenum Press: New York, 1991; pp 337−378.
(28) Eigen, M.; Rigler, R. *Proc. Natl. Acad. Sci. U.S.A.* **1994**, *91* (13), 5740−5747.
(29) Rigler, R.; Elson, E. S. *Fluorescence Correlation Spectroscopy: Theory and Applications*; Springer-Verlag: Berlin, 2001.
(30) Zander, C.; Enderlein, J.; Keller, R. A. *Single-Molecule Detection in Solution: Methods and Applications*; VCH−Wiley: Berlin/New York, 2002.
(31) Felekyan, S.; Kühnemuth, R.; Kudryavtsev, V.; Sandhagen, C.; Becker, W.; Seidel, C. A. M. *Rev. Sci. Instrum.* Accepted for publication.
(32) Widengren, J.; Rigler, R. *Cell. Mol. Biol.* **1998**, *44* (5), 857−879.
(33) Hess, S. T.; Huang, S.; Heikal, A. A.; Webb, W. W. *Biochemistry* **2002**, *41* (3), 697−705.
(34) Bacia, K.; Schwille, P. *Methods* **2003**, *29* (1), 74−85.
(35) Widengren, J.; Schweinberger, E.; Berger, S.; Seidel, C. A. M. *J. Phys. Chem. A* **2001**, *105* (28), 6851−6866.
(36) Widengren, J.; Dapprich, J.; Rigler, R. *Chem. Phys.* **1997**, *216* (3), 417−426.

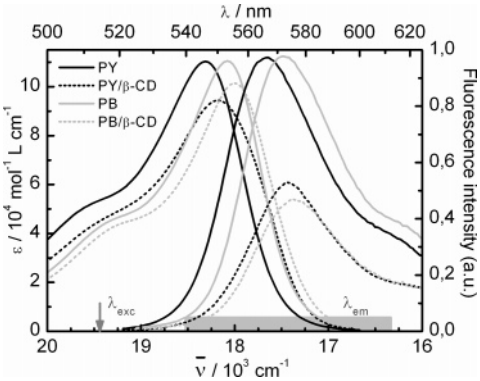

Figure 2. Absorption and fluorescence emission spectra of the free pyronines (solid lines) and of their complexes with β-CD (dashed lines). Black: PB, gray: PY. Also indicated are the excitation wavelength (λ_{exc} = 515 nm) and the range of detected emission wavelengths (λ_{em}) as determined by the band-pass filters used in the FCS measurements.

in two spectral ranges), which can be used to classify molecules into the different subpopulations that compose an ensemble and to characterize their size, identity, diffusion times, or local environment.[37−39] However, there can be found only very few applications of FCS to other fields, and especially no study has been published with respect to supramolecular dynamics. As we will show, FCS is perfectly suited for this task. It readily resolves dynamic processes in the ground state within a wide time window; at the fast end, it is only limited by the excitation−deactivation rate of the fluorophore ($\approx 10^9$ s^{-1}), and at the slow end, its limit is given by the residence time in the millisecond time range of the diffusing molecule in the sample volume.

As guest molecules, the dyes pyronine Y (PY) and pyronine B (PB) are studied (Figure 1). They provide simplified models of the xanthene skeleton of rhodamines and are also used in the labeling of proteins and cell organelles. In a previous photophysical study on the complexation of PY and PB with β-CD we found that the two pyronines form 1:1 complexes with β-CD.[5] Complexation causes a slight red shift of the emission spectra of the pyronines, but decreases significantly their fluorescence quantum yields and lifetimes (Figure 2. The association equilibrium constant of PB is much higher than that of PY (K(PB) = 2.0 × 10^3 M^{-1}, K(PY) = 0.38 × 10^3 M^{-1}).[5] This is a surprising result since it is presumed that the more bulky PB would show stronger steric hindrance than PY to enter into the β-CD cavity. Comparison of the photophysical properties of the pyronines in different solvents with those of the complexes suggested that there are important specific interactions of the pyronines with the electron-rich oxygens present in the interior of the CD cavity, stabilizing the complexes formed with PB more than PY. To confirm this hypothesis, we will compare the complexation dynamics of these pyronines and analyze the individual steps during association and dissociation.

Experimental Section

Materials. PY was purchased from Sigma (51% dye content) and PB from Aldrich (57% dye content). The main impurities of these materials are not water-soluble, so that they can be separated by filtration of the aqueous solutions.[40] β-Cyclodextrin (kindly supplied by Roquette Laisa España, SA) was recrystallized twice from water and dried in a vacuum oven. $HClO_4$ (Merck, p.a.) was used to control the pH of the solutions. Water was purified with a Milli-Q system.

Sample Preparation. Stock solutions of PY or PB were prepared by dissolving the commercial product in water and immediately filtering to separate the impurities. The absence of fluorescent impurities in these stocks was checked ensuring that the fluorescence excitation and emission spectra of diluted aqueous solutions do not differ for different emission and excitation wavelengths, respectively. Moreover, the presence of nonemitting impurities can be ruled out as the fluorescence excitation spectra match perfectly the corresponding absorption spectra down to the UV region. The potential influence of impurities on the results can be further excluded as very reproducible complexation equilibrium constants were obtained even for very different filtration conditions. The natural pH of these stocks was acid, in the range from 2.9 to 3.3, so that pyronine hydrolysis was very slow and the solutions were relatively stable within 2−3 days (kept protected from light).[5] The concentration of the stocks was determined using the reported values of molar absorptivities for PY[41] and for PB.[42]

Aqueous solutions for FCS measurements were freshly prepared from stock solutions by two dilution steps. First, the stock solutions were diluted with an aqueous $HClO_4$ solution of pH = 4.0 ± 0.2 to concentrations 10-times that of the final value. From these working stock solutions, the FCS samples of varying CD concentration were prepared by dilution of a constant volume of these pyronine stocks together with different volumes of a β-CD stock solution (concentration about 0.011 M) and the $HClO_4$ solution of pH = 4 as solvent. The final concentrations in the FCS samples were [PB] = 4 × 10^{-8} M and [PY] = 9 × 10^{-9} M. Poor reproducibility of absorbance and fluorescence intensity was observed for the aqueous solutions of PB without β-CD, which was attributed to the reported adsorption of pyronines on glass surfaces.[40,42] This problem was minimized by addition of small amounts of β-CD to the PB working stock solutions.

FCS Measurements. The principles of confocal setups for FCS measurements have been described elsewhere.[27,29,30,32,43] In the experimental setup used in this study, the fluorescent samples were excited by an argon ion laser beam (Coherent Innova, 515 nm). After reflection by a dichroic beam splitter (535 DCLP, AHF Analysentechnik Tübingen, Germany), the laser beam was focused into the sample by a microscope objective (Olympus 60X, NA 1.20, water immersion). The fluorescence was collected by the same objective and refocused to the image plane, where a pinhole (radius 100 μm) was placed. The two polarization components were separated by a polarizing cube and then individually detected by avalanche photodiodes (SPCM-AQR-14, Perkin-Elmer Vaudreuil, Quebec, Canada). Two band-pass filters (HQ575/70, AHF Analysentechnik) in front of the detectors discriminated fluorescence from laser light scattered at the excitation wavelength and from Raman scattered light of the solvent molecules. Both output signals were processed and stored by modified TCSPC modules (SPC 132, Becker & Hickl GmbH (Berlin, Germany)).[31] Correlation curves were calculated with a fast home-built routine which runs under LabVIEW (National Instruments).[31] Typically, 40 million photons were collected for each correlation curve with count rates between 50 and 350 kHz. All measurements were made at room temperature, stabilized at 21 °C. The excitation power of the laser beam was measured under the microscope objective by a power meter (Fieldmaster, model FM-2,Coherent). Excitation power in the sample volume was typically 290 μW, corresponding to a mean irradiation of $I_0/2 \approx 25$ kW/cm^2.[44]

(37) Kühnemuth, R.; Seidel, C. A. M. *Single Molecules* **2001**, *2* (4), 251−254.
(38) Eggeling, C.; Berger, S.; Brand, L.; Fries, J. R.; Schaffer, J.; Volkmer, A.; Seidel, C. A. M. *J. Biotechnol.* **2001**, *86* (3), 163−180.
(39) Rothwell, P. J.; Berger, S.; Kensch, O.; Felekyan, S.; Antonik, M.; Wöhrl, B. M.; Restle, T.; Goody, R. S.; Seidel, C. A. M. *Proc. Natl. Acad. Sci. U.S.A.* **2003**, *100* (4), 1655−1660.
(40) Schiller, R. L.; Lincoln, S. F.; Coates, J. H. *J. Chem. Soc., Faraday Trans. 1* **1987**, *83* (11), 3237−3248.
(41) Baraka, M. E.; Deumie, M.; Viallet, P.; Lampidis, T. J. *J. Photochem. Photobiol., A* **1991**, *56*, 295−311.
(42) Schiller, R. L.; Lincoln, S. F.; Coates, J. H. *J. Chem. Soc., Faraday Trans. 1* **1986**, *82*, 2123−2132.
(43) Krichevsky, O.; Bonnet, G. *Rep. Prog. Phys.* **2002**, *65*, 251−297.
(44) Eggeling, C.; Widengren, J.; Rigler, R.; Seidel, C. A. M. *Anal. Chem.* **1998**, *70* (13), 2651−2659.

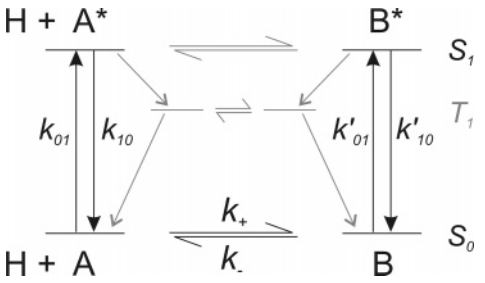

Figure 3. Proposed kinetic mechanism for the complexation of a guest A by a host H.

Calibration. The focal area and the detection volume have to be calibrated using a dye with known diffusion coefficient. Data from correlation measurements of Rh6G in aqueous solutions measured under the same conditions as all other samples are used in this study. For the diffusion coefficient, D(Rh6G), two values have been found in the literature: $(2.9 \pm 0.7) \times 10^{-10}$ m^2 s^{-1} from FCS data[45] and $(2.9 \pm 0.7) \times 10^{-10}$ m^2 s^{-1} measured by NMR,[46] both at 25 °C. The values show high uncertainties of about 25%, but coincide well in their mean value. All error intervals given in this work for values determined on the basis of these D(Rh6G) reference values indicate only their statistical error (*precision*) and do not include their *accuracy*, which is limited mainly by the uncertainty in the reference value. The precision is used for comparisons between values measured relative to the same reference value, whereas the accuracy has to be included when comparing these values with others measured with a different technique. The calibration with Rh6G at low irradiance yields a diffusion time of $\tau_D = 0.360 \pm 0.008$ ms that results in a radial $1/e^2$ radius of $w_{xy} = 0.61 \pm 0.01$ μm. All values were corrected for temperature and viscosity effects. All diffusion times, both of reference and samples, were measured at the same temperature. This way the effects of temperature and viscosity cancel each other out during the calibration, and all diffusion coefficients determined in this work refer thus to the temperature at which the D(Rh6G) reference value was given (25 °C).

We tried to avoid several experimental factors, which were recently identified to introduce significant errors in the determination of *absolute* diffusion coefficients.[47−49] (1) Saturation and photobleaching effects during the calibration measurements with Rh6G were avoided by reducing the irradiance far below saturation until no change was observed in the diffusion times and in the deduced sample geometry. (2) To minimize aberrations, the laser beam was not focused to the diffraction limit. In this way, the diffusion properties of the pyronines PY and PB obtained from correlation curves were independent of the irradiance.

Data Analysis. Two levels of nonlinear data analysis have been applied. (1) Individual correlation curves were fitted using the Levenberg−Marquardt algorithm programmed in LabVIEW (National Instruments).[31] (2) Series of correlation curves measured at different β-CD concentrations were analyzed by global "target" analysis programmed in OriginPro 7.0 (OriginLab Corporation).

Theory

Mechanism. Using the dye's fluorescence as a monitoring signal, the general kinetic mechanism for the complexation of a dye A by host H to form complex B would include all association/dissociation processes between the free and the complexed dye in the electronic ground state, singlet excited state, and triplet state (see Figure 3). However, under certain conditions, which are easily fulfilled, only ground state processes have to be taken into account. Bimolecular association rate constants are limited by diffusion ($k_+ \leq k_d \approx 10^9$ M^{-1} s^{-1}), and the concentration of the host [H] is limited by solubility ([β-CD]$_0 \lesssim 10^{-2}$ M). Thus, under pseudo-first-order conditions ([H]$_0 \approx$ [H] $\gg$ [A]), the association rate constant ($k_+ \times$ [H]$_0 \lesssim 10^7$ s^{-1}) is generally much smaller than typical decay rate constants of the excited singlet state of organic dyes ($k_{10} \approx 10^8-10^9$ s^{-1}) and can otherwise be reduced by lowering [H]$_0$. The dissociation rate constant k_-, on the other hand, can be estimated from the complexation equilibrium constant $K = k_+/k_-$. Even for a low value of $K = 100$ M^{-1} s^{-1} and the highest association rate constant, the dissociation is at most $k_- \leq 10^7$ s^{-1}, which is again well below typical values of the decay rate constant k_{10}. Thus, as long as the excitation rate is low enough, the relaxation of the singlet excited state is much faster than the ground state association/dissociation dynamics. At sufficiently low excitation energies and low intersystem crossing rate constants, the association/dissociation of the dye in its triplet state can be neglected, as well.

In this way, the resulting mechanism in Figure 3 reduces to the complexation equilibrium in the ground state, where both species are fluorescent. A similar reaction has been investigated by Widengren et al., who studied the complex formation of Rh6G by guanosine triphosphate.[36] They deduced a solution including the triplet-state population but simplified their system assuming a nonfluorescent complex, which is not suitable here.

FCS. FCS analyzes fluorescence intensity fluctuations which may be caused by changes in the excited singlet or triplet-state population, changes in concentration due to translational motion of the fluorophores in and out of the sample volume, or changes in their physicochemical properties, for example, due to a chemical reaction or, as in our case, complexation. The normalized autocorrelation function $G(\tau)$ of the intensity fluctuations $\delta I(t) = I(t) - \langle I \rangle$ indicates in this case the variation in the probability to register from the same molecule a second photon at the correlation time τ, once a first was emitted:

$$G(\tau) = \frac{\langle \delta I(t) \times \delta I(t+\tau) \rangle}{\langle I(t) \rangle^2} \tag{1}$$

If the fluorescence intensity fluctuations arise only from translational diffusion, the time-dependent part of the correlation function is given by:[43,50,51]

$$G_D(\tau) = \frac{1}{N}\left(1 + \frac{\tau}{\tau_D}\right)^{-1}\left(1 + \left(\frac{w_{xy}}{w_z}\right)^2 \frac{\tau}{\tau_D}\right)^{-1/2} \tag{2}$$

Here, a three-dimensional Gaussian distribution of the detected fluorescence is assumed. N is the mean number of fluorescent molecules within the sample volume, and τ_D is the translational diffusion time of the molecules across the sample volume. The translational diffusion coefficient D is related to τ_D by:

$$D = \frac{{w_{xy}}^2}{4\tau_D} \tag{3}$$

(45) Magde, D.; Elson, E. L.; Webb, W. W. *Biopolymers* **1974**, *13* (1), 29−61.
(46) Gell, C.; Brockwell, D. J.; Beddard, G. S.; Radford, S. E.; Kalverda, A. P.; Smith, D. A. *Single Molecules* **2001**, *2* (3), 177−181.
(47) Hess, S. T.; Webb, W. W. *Biophys. J.* **2002**, *83* (4), 2300−2317.
(48) Enderlein, J.; Gregor, I.; Patra, D.; Fitter, J. *Curr. Pharm. Biotechnol.* **2004**, *5* (2), 155−161.
(49) Krouglova, T.; Vercammen, J.; Engelborghs, Y. *Biophys. J.* **2004**, *87* (4), 2635−2646.
(50) Elson, E. L.; Magde, D. *Biopolymers* **1974**, *13* (1), 1−27.
(51) Rigler, R.; Mets, Ü.; Widengren, J.; Kask, P. *Eur. Biophys. J.* **1993**, *22* (3), 169−175.

The value of G_D at $\tau = 0$ gives the inverse of the number of fluorescent molecules $G_D(0) = 1/N$.

The diffusion time gives an upper limit for the time scale of observable processes. On the fast end, the rates of fluorescence excitation and emission limit the rate with which two successive photons from the same molecule can be detected. This introduces the antibunching term $G_F(\tau)$ with the characteristic rise time $\tau_F = (k_{01} + k_{10})^{-1}$, determined by the inverse of the sum of the excitation rate constant k_{01} and the decay rate constant of the excited state k_{10}, and an amplitude A_F:[52,53]

$$G_F(\tau) = (1 - A_F\, e^{-\tau/\tau_F}), \quad A_F = 1 \tag{4}$$

Triplet-state formation leads to an additional term $G_T(\tau)$ in the correlation function with a characteristic triplet time τ_T and an amplitude A_T, which is related to the fraction of molecules, T, being trapped in the "dark" triplet state in the excitation cycle.[54,55] In the simplest case, the triplet-state formation is taken as being independent from all other processes:

$$G_T(\tau) = (1 + A_T\, e^{-\tau/\tau_T}), A_T = \frac{T}{1-T} \tag{5}$$

So finally, under the condition $\tau_D \gg \tau_T \gg \tau_F$, these processes are described in FCS by a correlation function which is the product of the individual functions from eqs 2, 4, and 5:

$$G(\tau) = G_F \times G_T \times G_D \tag{6}$$

General Correlation Function for a Chemical Equilibrium Reaction. The association of fluorescent guest A and a nonfluorescent host H yielding a fluorescent complex B is treated as a chemical reaction with (association) equilibrium constant K:

$$A + H \overset{K}{\rightleftharpoons} B, \quad K = \frac{k_+}{k_-} \tag{7}$$

with the association rate constant k_+ and the dissociation rate constant k_-. Under the conditions used in this study, the free host concentration is always much higher than that of the guest, [H] $\gg$ [A], and can be approximated by the total host concentration, [H] $\approx$ [H]$_0$. Then, the reaction is of pseudo-first-order with the relaxation time, τ_R, which is given by the inverse sum of the association and dissociation rate constants:

$$\tau_R = (k_+ [H]_0 + k_-)^{-1} \tag{8}$$

For certain experimental conditions, special solutions for the correlation function $G_R(\tau)$ of this reaction have been published before. Elson and Magde derived a general solution for $G_R(\tau)$ for a unimolecular isomerization, supposed, however, a cylindrical sample volume illuminated by a laser beam with Gaussian intensity profile.[50] This solution has been simplified for the case that the diffusion coefficients of A and B do not change during reaction ($D_A = D_B$).[50,56] For this special case, the solution for

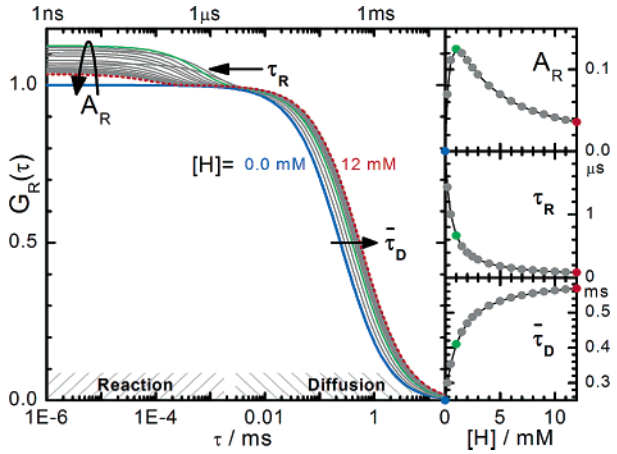

Figure 4. Main panel: Simulated correlation curves illustrating the variation of $G_R(\tau)$ with increasing host concentration $[H]_0$ following eqs 9, 11, 12, and 13. Side panels: Dependence of A_R, τ_R, and $\bar{\tau}_D$ on host concentration $[H]_0$. Parameters used for the simulation: $N_A + N_B = 1$, $\tau_A = 0.25$ ms, $\tau_B = 0.60$ ms, $w_z/w_{xy} = 5$, $K = 2000$ M^{-1}, $Q = 0.5$, and $k_- = 5 \times 10^5$ s^{-1}.

Gaussian illumination in a confocal setup has been given.[27,43,57,58] Widengren et al. deduced a solution including the triplet-state population but simplified their system supposing a nonfluorescent complex.[36]

In our case, a new general solution is derived which describes two interconverting fluorescent species with different diffusion coefficients observed under Gaussian illumination. Extending the solution of Elson and Magde to confocal Gaussian illumination, introducing the mean diffusion time,[59] $\bar{\tau}_D$, and applying the assumption that the relaxation rate of the reaction is much faster than the typical diffusion times of guest and complex (fast exchange, $\tau_R \ll \tau_A$, τ_B), the following correlation function is obtained:

$$G_R(\tau) = \frac{1}{N_A + N_B}\left(1 + \frac{\tau}{\bar{\tau}_D}\right)^{-1}\left(1 + \left(\frac{w_{xy}}{w_z}\right)^2 \frac{\tau}{\bar{\tau}_D}\right)^{-1/2}(1 + A_R e^{-\tau/\tau_R}) \tag{9}$$

with the mean diffusion time $\bar{\tau}_D$, the relaxation time τ_R, the amplitude of the reaction term A_R, and the mean numbers N_A and N_B of free guest and complex in the sample volume. The expression for the reaction term is in agreement with the two published borderline cases: (i) interconverting species with equal diffusion coefficients, and (ii) noninterconverting species with different diffusion coefficients.[27,56−58]

Properties of the Correlation Function $G_R(\tau)$. The properties of this correlation function are illustrated with simulated curves in Figure 4. The inserts indicate the dependencies of $\bar{\tau}_D$, τ_R, and A_R on the host concentration $[H]_0$.

Due to the condition of fast exchange during the dwell time of the molecule in the observation volume, only one averaged diffusion term is observed with the mean diffusion time $\bar{\tau}_D$ and an amplitude $N^{-1} = (N_A + N_B)^{-1}$, which yields directly the mean total number N of guest molecules in the sample volume. N does not depend on the brightness of the dyes or whether

(52) Mets, Ü. In *Fluorescence Correlation Spectroscopy: Theory and Applications*; Rigler, R., Elson, E. S., Eds.; Springer-Verlag: Berlin, 2001; Vol. 65, pp 346−359.
(53) Kask, P.; Piksarv, P.; Mets, Ü. *Eur. Biophys. J.* **1985**, *12* (3), 163−166.
(54) Widengren, J.; Mets, Ü.; Rigler, R. *J. Phys. Chem.* **1995**, *99* (36), 13368−13379.
(55) Widengren, J. In *Fluorescence Correlation Spectroscopy: Theory and Applications*; Rigler, R., Elson, E. S., Eds.; Springer-Verlag: Berlin, 2001; Vol. 65, pp 276−301.
(56) Palmer, A. G., III; Thompson, N. L. *Biophys. J.* **1987**, *51*, 339−343.
(57) Widengren, J.; Terry, B.; Rigler, R. *Chem. Phys.* **1999**, *249* (2−3), 259−271.
(58) Malvezzi-Campeggi, F.; Jahnz, M.; Heinze, K. G.; Dittrich, P.; Schwille, P. *Biophys. J.* **2001**, *81* (3), 1776−1785.
(59) Berne, B. J.; Pecora, R. *Dynamic Light Scattering*; Robert E. Krieger Publishing Company: Malabar, FL, 1990.

they are free or complexed. The amplitude N^{-1} corresponds to the total amplitude in the cases where $A_R = 0$.

The mean diffusion time $\bar{\tau}_D$ depends on the number-weighted mean diffusion coefficient $\bar{D}$ obtained from the individual coefficients D_A and D_B:

$$\bar{\tau}_D = \frac{w_{xy}^2}{4\bar{D}}, \quad \bar{D} = X_A D_A + X_B D_B \tag{10}$$

with the fractions $X_x = N_x/(N_A + N_B)$.[59] In the limiting case of $D_A = D_B$, no variation of $\bar{\tau}_D$ will be observed. For the subsequent analysis of a titration series with varying host concentration $[H]_0$, it is advantageous to express $\bar{\tau}_D$ directly as a function of the host concentration $[H]_0$ and the association equilibrium constant K (eq 7):

$$\bar{\tau}_D([H]) = \frac{\tau_A(1 + K[H]_0)}{1 + \frac{\tau_A}{\tau_B}K[H]_0} \quad \text{with } \tau_x = \frac{w_{xy}^2}{4D_x}, \quad \frac{D_B}{D_A} = \frac{\tau_A}{\tau_B} \tag{11}$$

With increasing $[H]_0$, the observed diffusion time $\bar{\tau}_D$ shifts from τ_A to τ_B (Figure 4, right panel).

The relaxation time τ_R (eq 8) of the reaction term can be expressed as a function of the equilibrium constant K. It decreases with increasing host concentration $[H]_0$:

$$\tau_R([H]) = (k_-(1 + K[H]_0))^{-1} \tag{12}$$

The amplitude of the reaction term A_R (Figure 4, left panel) depends on two factors:

$$A_R = \frac{N_A N_B (Q_A - Q_B)^2}{(Q_A N_A + Q_B N_B)^2} = \frac{K[H]_0(1 - Q)^2}{(1 + QK[H]_0)^2} \tag{13}$$

(1) The ratio between the brightnesses, $Q = Q_B/Q_A$, of free guest A and the complex B. The species-dependent brightness is defined by the product of the extinction coefficients, fluorescence quantum yield, and detection efficiency, $\epsilon_x \Phi_{(F)x} g_x$.

(2) The concentration of both species. The amplitude of the reaction term vanishes both at very low and at very high host concentrations $[H]_0$, that is, when $N_B = 0$ or $N_A = 0$, respectively.

The value of $G_R(\tau)$ for $\tau \rightarrow \infty$ is zero, and the value at $\tau = 0$ depends both on the number of fluorescent molecules and on their brightnesses:

$$G_R(0) = \frac{N_A Q_A^2 + N_B Q_B^2}{(Q_A N_A + Q_B N_B)^2} \tag{14}$$

Analogous to eq 6, the complexation equilibrium relaxation is taken to be independent from antibunching and triplet-state formation (see Figure 3), and thus the complete correlation function is given by the product of individual correlation functions given in eqs 4, 5, and 9:

$$G(\tau) = G_F \times G_T \times G_R \tag{15}$$

Results and Discussion

FCS of Free Dyes. The normalized fluorescence correlation curve of an aqueous solution of PY is shown as the heavy black line in Figure 5. It presents a fast increase of $G(\tau)$ in the range from 1 to 10 ns, then a nearly constant plateau up to 10 μs, and finally a strong decrease to 0 at longer correlation times. PB shows a very similar behavior. These correlation curves of PY and PB are perfectly fitted in the whole region between 1 and 100 ms with the correlation function (eq 6); the different regions described before correspond thus to the terms for antibunching G_F, triplet-state formation G_T, and diffusion G_D, respectively. The diffusion times obtained for PY and PB are $\tau_D = 0.251 \pm 0.001$ ms and $\tau_D = 0.31 \pm 0.03$ ms, respectively. The triplet terms around $\tau_T = 1$ μs present in both cases very low amplitudes of about $A_T = 0.02$. The rise time of the antibunching terms $\tau_F = 2 \pm 1$ ns obtained for PY and PB coincides well with their known fluorescence lifetimes of 1.8 and 1.3 ns, respectively.[5] During the measurements, the excitation rate $k_{01} \approx 10^7$ s^{-1} was kept so low that the rise time, $\tau_F = (k_{01} + k_{10})^{-1}$, is determined by the lifetime of the excited state, $\tau_F \approx k_{10}^{-1}$. It must be noted that the FCS setup used for these measurement would have allowed one to determine the rise time with much higher precision, but this is not the aim of this study.

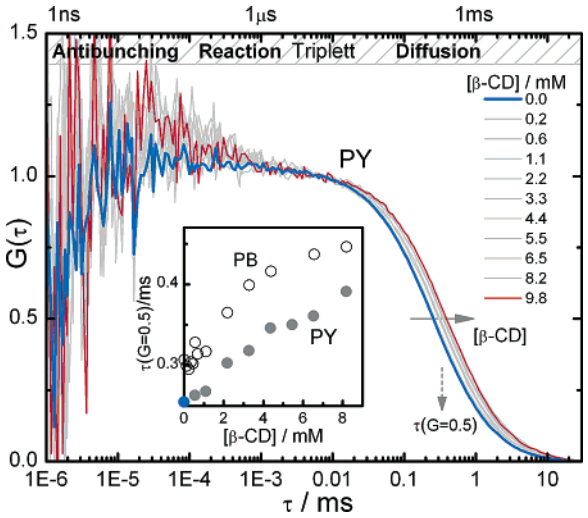

Figure 5. Normalized correlation curves of PY in water measured with increasing concentrations of β-CD as indicated in the figure. (Normalization: $G(0.006\text{ ms}) = 1.0$.) Inset: Correlation times at half-height of the normalized diffusion term $\tau(G = 0.5)$ versus β-CD concentration. Filled circles: PY; open circles: PB.

FCS of Dyes with β-CD. On the addition of β-CD, the correlation curves of PY and PB show two significant changes (Figure 5): (1) the diffusion term shifts to increasingly longer correlation times. The plot of the correlation times at half-height of the normalized diffusion term $\tau(G = 0.5)$ as function of the β-CD concentration (inset in Figure 5) indicates that the initial increase in the diffusion time $\tau(G = 0.5)$ is faster for PB than for PY; (2) additionally to the terms described before, a new (bunching) term appears at intermediate correlation times which shifts to shorter correlation times with increasing β-CD concentration. Its amplitude increases first rapidly and decreases at higher β-CD concentrations (see also Figure 6).

These changes can be perfectly explained by the complexation of the pyronines with β-CD as predicted by the simulations in Figure 4: (1) the molar mass of the formed complex is about 5 times higher than that of the free guest fluorophore, and consequently, the observed mean diffusion time increases approximately from 0.25 to 0.40 ms for PY and from 0.30 to 0.45 ms for PB as more complex is formed; (2) the difference

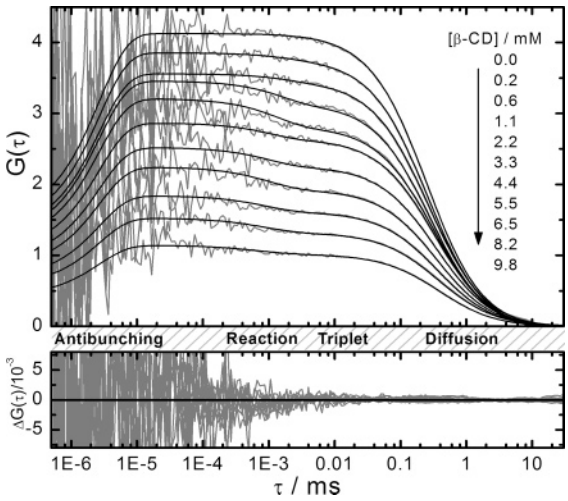

Figure 6. Correlation curves of PY in water measured with increasing concentrations of β-CD as indicated in the figure. Gray lines are experimental curves, normalized ($G(0.006\ \text{ms}) = 1.0$), and then arbitrarily scaled in order to separate them visually. Black lines are theoretical curves determined by global target fits of eq 15 to the experimental curves, as explained in the text. The parameters obtained in the fit are given in Table 1.

in brightness of free and complexed fluorophore[5] together with the fast formation and dissociation of the complex during the dwell time of the fluorophore in the observation volume results in a "reaction term" in the correlation curve with a typical correlation time given by the relaxation rate of the complexation process in the range from 0.1 to 1 μs.

Analysis of FCS Data. The separate analysis of the diffusion terms of the individual curves presents certain difficulties. Due to the low association constant of the pyronines and to the relatively poor solubility of β-CD in water, even at the highest β-CD concentration about 20% of the PY molecules are still free. Thus, the diffusion time of the complex τ_B cannot be directly determined. The attempts to determine the diffusion time τ_B and the association constant K from the dependence of $\bar{\tau}_D(\beta\text{-CD})$ on the β-CD concentration determined from individual fits of the diffusion terms leads to values of τ_B and K with high uncertainty and a mean value for K which is significantly smaller than that reported before.[5] This is mainly due to strong statistical parameter correlations between K and τ_B.[60] Moreover, the analysis of individual correlation curves with the full correlation function (eq 15) fails because of strong statistical correlations among the fit parameters.

Global Target Analysis of FCS Data. To make the best use of the experimental data and to reduce parameter correlations, all curves were analyzed together in a global "target" fit,[61] taking the dependence of some of the fit parameters on the β-CD concentration into account. The concentration-dependent parameters, such as the mean diffusion time $\bar{\tau}_D$, the reaction relaxation time τ_R, and the reaction term amplitude A_R, were recalculated at each iteration from the global parameters of interest such as the diffusion times of free and complexed guests τ_A and τ_B, the brightness ratio Q, the association constant K, and the complex dissociation rate constant k_-, using eqs 11−13. Additional parameters, such as the triplet relaxation time τ_T, the rise time τ_F, and the geometry factor of the observation volume w_z/w_{xy}, are known from the calibration measurements and were fixed at their known values during the global target analysis.

Table 1. Results from Global "Target" Fits of Equation 15 (see text) to a Series of Correlation Curves Measured at Different β-CD Concentrations, Both with Free and Fixed Values of K. In all cases fixed values were used for $w_z/w_{xy} = 5.2$, $\tau_T = 1.5\ \mu$s, and $\tau_F = 2$ ns; $Q = Q_B/Q_A$; reference values were published previously[5]

	τ_A (ms)	τ_B (ms)	K ($\times 10^3\ M^{-1}$)	Q	k_- ($\times 10^4\ s^{-1}$)
PY	0.25 ± 0.02	0.46 ± 0.13	0.36 ± 0.55	0.6 ± 0.2	50 ± 80
	0.25 ± 0.02	0.45 ± 0.06	0.4 fixed	0.6 ± 0.2	50 ± 30
ref			0.40 ± 0.04	0.50	
PB	0.30 ± 0.02	0.42 ± 0.06	1.2 ± 0.9	0.48 ± 0.12	9.5 ± 8.4
	0.30 ± 0.02	0.40 ± 0.04	2 fixed	0.49 ± 0.04	7.6 ± 2.7
ref			2.1 ± 0.2	0.49	

Thus, the global parameters τ_A, τ_B, w_z/w_{xy}, K, τ_T, Q, k_-, and τ_F were shared between all correlation curves, whereas the (linear scaling) parameters such as the mean molecule number $N = N_A + N_B$ and the triplet term amplitude A_T were varied individually with each measurement. No weighting of the data was applied for the fit procedure. The fit was started by fixing the global parameters at guessed initial values, which were then released one by one in successive runs. This procedure assured that a meaningful minimum was found in a reasonable time. The values of the directly fitted parameters are given in Table 1.

The corresponding fit curves are represented in Figure 6 for PY. The curves for PB are very similar. Leaving K free in the analysis leads to a value for K(PY), which is in good agreement with the value reported by Reija et al.[5] The big given uncertainty, however, indicates strong statistical correlation with other parameters, especially with τ_B and k_-. Fixing K to the reported value reduces the uncertainties of the other parameters without changing significantly their fitted values (see Table 1). The amplitudes of the triplet terms A_T were always below 0.02. Considering the spectral properties of the detection system and the specific fluorescence quantum yields, the estimated ratios of the brightnesses $Q = Q_B/Q_A$ are in very good agreement with the data determined from bulk measurements $Q(\text{PY}) = 0.50$ and $Q(\text{PB}) = 0.49$.[5]

At this point, FCS already demonstrates its great potential to determine the rate constants of the association/dissociation process together with valuable information about diffusional properties. These results are discussed in the following sections.

Translational Diffusion Coefficients. The diffusion times determined from the fluorescence correlation curves were converted to translational diffusion coefficients using eq 3 with the radial $1/e^2$ radius of the measurement volume w_{xy} obtained from a calibration with Rh6G as a standard (see Experimental Section). The hydrodynamic radius R_h was calculated applying the Stokes−Einstein relation

$$R_h = \frac{kT}{6\pi\eta D} \tag{16}$$

with the viscosity $\eta(25\ ^\circ\text{C}) = 0.8905$ cP of water (see Table 2). All values are corrected for a temperature of 25 °C.

The free guests PY and PB show the highest diffusion coefficients, D, where D(PB) is significantly lower than D(PY) (see Table 2). Their inclusion complexes with β-CD have much smaller diffusion coefficients which, however, are not signifi-

(60) Johnson, M. L. *Methods Enzymol.* **2000**, *321*, 424−446.
(61) Beechem, J. M.; Ameloot, M.; Brand, L. *Chem. Phys. Lett.* **1985**, *120* (4−5), 466−472.

Table 2. Diffusion Coefficients and Hydrodynamic Radii Calculated from the Diffusion Times Given in Table 1 and Equations 3 and 16. All Values Corrected for 25 °C. Molar Mass (M_w) Is Given for Comparison and Does Not Include the Counterions for the Charged Dyes. Uncertainties Do Not Include Calibration Errors

	D ($\times 10^{-10}$ m^2 s^{-1})	R_h (Å)	M_w (Da)
PY	4.2 ± 0.3	5.8 ± 0.4	267
PY:β-CD	2.4 ± 0.3	10 ± 1	1402
PB	3.5 ± 0.3	7.0 ± 0.6	324
PB:β-CD	2.6 ± 0.3	9 ± 1	1459
β-CD	$(3.23 \pm 0.07)^a$	7.6 ± 0.3	1135
Rh6G	$(2.9 \pm 0.7)^b$	9 ± 2	443
Rh110	3.4 ± 0.3	7.2 ± 0.6	331
P110	$(4.7)^c$	5	211

[a] NMR data (ref 62). [b] NMR data (ref 46). [c] Diffusion limit in fluorescence quenching experiments (ref 63).

cantly different. The literature value for the diffusion coefficient of β-CD falls between the values for the free guests and the complexes.

These results reflect qualitatively the different steric dimensions of the molecules involved. The free guest PY is the smallest, followed by PB, β-CD, and then the complexes. The increase in size from PY to PB, due to the exchange of the methyl groups by ethyl groups, affects the diffusional properties of the free dyes, but not those of the much bigger inclusion complexes formed. The derived hydrodynamic radii of PY and PB correspond well to geometric dimensions estimated from molecular models. The hydrodynamic radii of the complexes are very similar for both types of complexes, and somewhat larger than that of β-CD alone.

Variation of the Diffusion Coefficients with Molar Mass. For a more detailed analysis, the dependence of the diffusion coefficients, D, on the molar mass is analyzed. Applying the Stokes−Einstein relation (eq 16), the diffusion coefficient of homogeneous spherical particles is expected to change with their molar mass following a power law (allometric scaling) with exponent −1/3: $D \sim R_h^{-1} \sim M_w^{-1/3}$. Figure 7 shows a double logarithmic plot of D values versus molar mass M_w for the molecules studied here and for some literature values of other guests without charge, cyclodextrins of other sizes, and cyclodextrin complexes.

The literature values of the neutral molecules show in the double logarithmic plot an excellent linear correlation. Fitting the power law

$$D = a \times M_w^{-\nu} \qquad (17)$$

to the data yields an exponent $\nu = 0.399 \pm 0.003$ (dashed line in Figure 7). This value lies slightly above the value of $\nu = 1/3$ expected for homogeneous spheres. Random coils of polymer chains would show $\nu = 1/2$, rigid rods $\nu = 1$.[65] This indicates very similar diffusional properties of the small sugars, the steroid guest, the cyclodextrin hosts, and the complexes formed between steroid and hosts, all scaling with molar mass as expected for

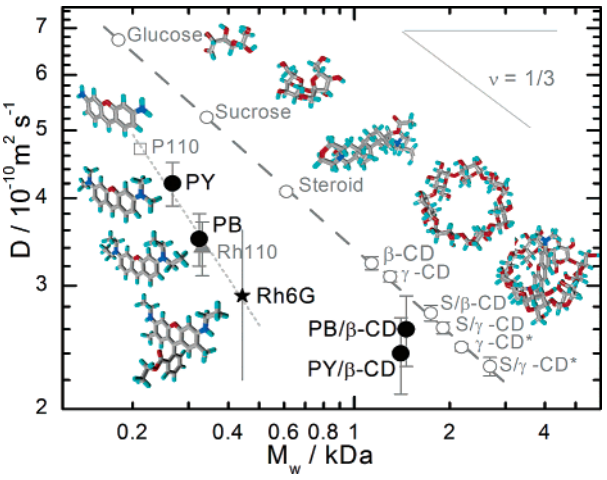

Figure 7. Double logarithmic plot of translational diffusion coefficients D versus molar mass. Filled circles: Experimental values of PY and PB and their complexes with β-CD from Table 2. Star: Reference value of Rh6G (NMR data[46]). Gray triangle: Value for rhodamine 110 determined by FCS in the same way as PY and PB. Open square: Value for pyronine 110 determined from fluorescence quenching experiments.[63] Open circles: Literature values (glucose, sucrose,[64] steroid, CDs, and steroid/CD complexes from NMR data[62]). Dashed line: Fit of eq 17 to literature values (open circles) with $\nu = 0.399 \pm 0.003$. Dotted line: Fit of eq 17 to PY, PB, P110, Rh110, and Rh6G values with $\nu = 0.7 \pm 0.1$. The error bar at the reference Rh6G value indicates ±25% accuracy, which is not included in the error bars of the other values. All values are given for 25 °C. The molar masses of the charged dyes do not include the counterions.

nearly homogeneous compact spheres. It is especially remarkable that the hollow cyclodextrins fit perfectly in this scheme, indicating that their interior is essentially undrained during diffusion.

The literature value for D(Rh6G), however, falls much below this group of data, although it was determined by the same NMR technique as the steroid/cyclodextrin data.

The diffusion coefficients of the pyronine guests PY and PB and of the dyes pyronine 110 (P110) and rhodamine 110 (Rh110) show the same tendency as that of Rh6G. Being the pyronines models of the xanthene skeleton of the rhodamines, one may tentatively fit the allometric model through these values (dotted line in Figure 7). The resulting exponent of about $\nu = 0.7 \pm 0.1$ indicates strong deviation from the spherical homogeneous mass distribution, which would be in concordance with the much more planar configuration of the aromatic structure of these dyes as compared to the more compact globular configuration of the sugars and steroid complexes analyzed before. It also has to be considered that all dyes of this group bear a single positive charge. This increases their hydrated volumes and thus reduces their diffusion coefficients.

Diffusion Coefficients of Host−Guest Complexes. A different behavior is found for the inclusion complexes between the pyronines and β-CD, which show similar diffusion coefficients close to that of the steroid:CD complexes. This finding indicates that the differences in shape observed for the different guests become less important once the guests are included in the host. The resulting inclusion complexes are all roughly globular with a similar mass distribution. The effect of the single charge of the included guest on the hydrated volume of the whole complex should also be smaller than that in the case of the free guest.

Complexation Dynamics. The values obtained from the global analysis of the FCS curves for the dissociation (k_-) and

(62) Cameron, K. S.; Fielding, L. *Magn. Reson. Chem.* **2002**, *40* (special issue), S106−S109.
(63) Fries, J. R. Charakterisierung einzelner Moleküle in Lösung mit Rhodamin-Farbstoffen. Ph.D Thesis, Universität-Gesamthochschule Siegen, Cuvillier, Göttingen, 1998.
(64) Weast, R. C. *CRC Handbook of Chemistry and Physics*; CRC Press: Boca Raton, FL, 1986.
(65) Burchard, W. In *Physical Techniques for the Study of Food Biopolymers*; Ross-Murphy, S. B., Ed.; Blackie Academic & Professional: London, 1994; pp 151−213.

Table 3. Rate Constants of the Association between Pyronines and β-CD. The Values of the Association Rate Constants k_+ Are Calculated from the k_- Given in Table 1 Using Equation 7 (with fixed K). The Rate Constants k_d, k_{-d}, and k_r Have Been Estimated Applying Bimolecular Reaction Theory Using the Equations 18, 20, 22, and 23 and the Values from Tables 1 and 2

	k_+ ($\times 10^9$ M^{-1} s^{-1})	k_d ($\times 10^9$ M^{-1} s^{-1})	k_{-d} ($\times 10^9$ s^{-1})	k_r ($\times 10^9$ s^{-1})	k_{-r} ($\times 10^4$ s^{-1})
PY	0.2 ± 0.1	7.5 ± 0.5	1.7 ± 0.1	0.05 ± 0.02	50 ± 30
PB	0.15 ± 0.05	7.4 ± 0.5	1.3 ± 0.1	0.03 ± 0.01	7.6 ± 2.7

association (k_+) rate constants of PY and PB with β-CD are listed in Tables 1 and 3. As pointed out before, the association/dissociation rates are not high enough to compete with the excited state deactivation processes of the free pyronines and the pyronine:CD complexes, even at the highest achievable concentrations of β-CD. This is in concordance with the proposed mechanism (Figure 3), in which no association/dissociation processes in the singlet excited state were considered.

Association. The values of the association rate constants k_+ of PY and PB coincide within experimental error (Table 3). In view of the bulkier ethyl groups of PB as compared to the smaller methyl groups of PY, this is, at first sight, a surprising fact; the increased steric volume of PB reduces both its diffusion coefficient and its probability to enter the CD cavity. The values of the association rate constants k_+ of PY and PB are among the highest association rate constants reported for a series of aromatic and aliphatic guests in the ground state[4] and are of the same order as those determined for bicyclic azoalkanes by Nau and co-workers.[25] Nevertheless, the association process is clearly not diffusion-controlled. Using the diffusional properties (D and R_h) determined by FCS before, the rate constants k_d for a purely diffusion-controlled association process can be estimated applying the Smoluchowski equation for the reaction between guest A and host H[66]

$$k_d = 4\pi D_{AH} R_{AH} N_0 \tag{18}$$

($D_{AH} = D_A + D_H$, $R_{AH} = R_A + R_H$, and N_0 is the Avogadro constant.) The calculated values k_d for the two pyronines are very similar (see Table 3). It is interesting to note that in eq 18 the effect of the different diffusion coefficients D_A of PY and PB is mostly compensated by the difference between their radii R_A (see Table 2).

Encounter Complex Formation. The diffusion-limited rate constants k_d are much higher than the observed association rate constants k_+, which are obviously limited by other processes than the diffusion itself. To elucidate the rate-determining steps, we describe the complexation as a two-step process, applying theory of bimolecular reactions used in electron transfer or quenching theory:[67−69]

$$A + H \underset{k_{-d}}{\overset{k_d}{\rightleftharpoons}} [A\cdot H] \underset{k_{-r}}{\overset{k_r}{\rightleftharpoons}} B \tag{19}$$

Due to diffusion, guest A and host H eventually get into contact with the diffusion-limited rate constant k_d (eq 18) to form an *encounter complex* [A·H], where A and H are within the same solvent cage. The formed encounter complex dissociates with the rate constant k_{-d}, which can be estimated from the time needed for guest and host to diffuse at least their molecular radii R_{AH} apart. This diffusion time can be deduced from eq 3 yielding

$$(k_{-d})^{-1} \approx \frac{R_{AH}^{\ 2}}{4D_{AH}} \tag{20}$$

The values k_{-d} of PY and PB differ by approximately 30% (see Table 3). The smaller value for PB is due to the fact that now both the lower diffusion coefficient and the larger radius of PB increase the corresponding encounter complex lifetime $(k_{-d})^{-1}$.

Thus, the ratio k_d/k_{-d} depends only on the volume occupied by host and guest and scales with the third power of the radius R_{AH}:

$$\frac{k_d}{k_{-d}} = \pi R_{AH}^{\ 3} N_0 \tag{21}$$

Inclusion Equilibrium. Once host and guest are in contact, the inclusion complex B may be formed with the "reaction rate constant" k_r. The rate constant k_{-r} describes the back reaction of the complex to the encounter pair.

In terms of this model, we may separate the overall complexation equilibrium into a pre-equilibrium between free molecules and the encounter complex with $K_{enc} = k_d/k_{-d}$ and the inclusion equilibrium with $K_r = k_r/k_{-r}$ between encounter complex and inclusion complex:

$$K = K_{enc}K_r = \frac{k_+}{k_-} = \frac{k_d}{k_{-d}} \times \frac{k_r}{k_{-r}} \tag{22}$$

With the values given in Table 3, we estimate from the ratio k_d/k_{-d} an encounter complex equilibrium constant K_{enc} of about 5 M^{-1} for both pyronines. With the known overall equilibrium constants K (Table 1), the inclusion equilibrium constants K_r(PY) = 90 and K_r(PB) = 350 can be calculated. Both K_r values show that the formation of the complex with k_r is much faster than the dissociation k_{-r}. This justifies neglecting k_{-r} in the kinetic description of k_+. Assuming steady-state conditions for the concentration of [A·H], the observed rate constant k_+ of formation of B can be expressed as

$$k_+ = k_r \frac{k_d}{k_{-d} + k_r} = \frac{k_d}{1 + \frac{k_d}{k_r}\frac{k_{-d}}{k_d}} \leftrightarrow k_r = \frac{k_+ k_{-d}}{k_d - k_+} \tag{23}$$

which allows one to estimate the unimolecular rate constant k_r of complex formation.

The different values of k_r (Table 3) indicate that PY has only a slightly higher probability than PB to form the complex during the lifetime of its encounter pair. This advantage, however, is in part eliminated by the shorter lifetime of the encounter pair of PY, so that the overall association rate

(66) Caldin, E. F. *The Mechanisms of Fast Reactions in Solution*; IOS Press: Amsterdam, 2001.
(67) Eigen, M. *Z. Phys. Chem. (Leipzig)* **1954**, *NF1*, 176.
(68) Eberson, L. In *Advances in Physical Organic Chemistry*; Gold, V., Bethell, D., Eds.: Academic Press: London, 1982; Vol. 18, pp 79−185.
(69) Valeur, B. *Molecular Fluorescence: Principles and Applications*; Wiley-VCH: Weinheim, Germany, 2002.

constants k_+ of PY and PB show no significant difference. The compensational effect between reaction rate and encounter lifetime may also explain to some extent the very similar association rate constants found by other authors for guest molecules of smaller size and the small influence different substitutions have on this constant.[25]

Influence of Steric Hindrance. The low ratios $k_r/k_{-d} \approx 0.02$ for PY and PB show that only about 2% of the formed encounter pairs actually lead to an inclusion complex. Can steric hindrance explain this low ratio? Applying a simple model used in bimolecular reactions, one may assume that during contact, host and guest collide and rotate due to brownian motion, but only those collisions in which both molecules are in favorable relative orientations are successful and give rise to an inclusion complex.[66] If during the lifetime of the encounter complex, N_{coll} collisions take place, the "reaction probability" P_r for inclusion complex formation during each of the collisions is equal to

$$P_r = \frac{1}{N_{coll}} \frac{k_r}{k_r + k_{-d}} \approx \frac{1}{N_{coll}} \frac{k_r}{k_{-d}} \qquad (24)$$

The number of collisions N_{coll} may be estimated roughly assuming that the molecules within the solvent cage have a mean speed similar to that in the gas phase (see the Supporting Information).[66] From kinetic gas theory, we estimate that during the lifetime of the encounter complex, host and guest collide on the order of $N_{coll} \approx 100$ times. This results in a probability to form an inclusion complex at each collision of about $P_r \approx 2 \times 10^{-4}$.

We estimated the fraction f_r of successful collisions by stepping systematically over all possible relative orientations and rotations between host and guest and deciding in each case whether the guest would fit geometrically into the opening presented by the cavity of the host (see the Supporting Information). This worst-case simulation yields some lower limit for the restrictions imposed by the orientational requirements but does not take into account any specific interactions or the flexibility of the molecules, which may allow an induced fit. Furthermore, we approximated the critical dimensions of the molecules by rectangular prisms representing the outline of the host and the cavity of the guest. Using the known geometric sizes of the pyronines and β-CD, the simulations indicated two interesting results: (1) the pyronines fit only very tightly into the β-CD cavity (see also Figure 1). As expected, the fraction f_r depends sensibly on the difference between the widths of guest and host. Assuming a gap of about 0.5 Å, only a fraction $f_r \approx 10^{-4}$ of the collisions are successful. This value agrees well with the observed reaction probability P_r. Increasing this critical gap by 1 Å increases f_r by a factor of 10. This coincides with the strong dependence generally found for the complexation properties on the inner diameter of the cyclodextrin used. (2) PY and PB are represented in the simulation by rectangular prisms with different width of their shortest side, reflecting the different alkyl residues of the pyronines. The width of this shortest side is always much smaller than the diameter of the β-CD cavity, and thus, a variation of this width has only a small influence on the fraction f_r. Increasing the width of the shorter side by 1 Å reduces f_r only by a factor of 2−3. This explains well the small variation in the values of the inclusion rate constant k_r found for PY and PB (see Table 3).

Despite the limitations that these simulations have, they indicate that the geometrical reorientation may be the rate-determining step in the inclusion process and that the rate of inclusion may be dictated by steric effects.

Dissociation. As opposed to the very similar association rate constants, a big difference is observed between the dissociation rate constants k_-, being the value for PY about 6 times higher than that for PB (see Table 3). This implies that the much higher stability of the PB:β-CD complex is mainly due to its slower dissociation process. Analogous results can be found in the literature, for example, for the already mentioned bicyclic azoalkanes[25] or for the isomers 1-naphthyl-1-ethanol and 2-naphthyl-1-ethanol, where the position of the substituent that allows the molecule to penetrate more or less deeply into the β-CD cavity has a strong effect on the dissociation rate constant but less on the association rate constant.[2]

From eqs 22 and 23 and $k_{-d} \gg k_r$, it is easy to see that the overall dissociation rate constant k_- is limited by the rate constant k_{-r}, with which the guest leaves the host forming again an encounter complex, and that this is the slowest of all involved steps.

The much lower dissociation rate constant of the PB:CD complex as compared to that of PY:CD confirms that PB interacts much stronger with the interior of the β-CD cavity. This was previously proposed on the basis of steady-state and time-resolved fluorescence studies[5] but could not be confirmed without information on the complexation dynamics. Specific interactions between the positively charged xanthene moiety of the pyronines and the electron-rich glucosidic oxygens of the β-CD cavity stabilize probably the inclusion complexes of both pyronines, but seem to be much stronger in the case of PB.

Acknowledgment. B.R. thanks the Ministerio de Educación y Ciencia for a research scholarship. M.N. and W.A. thank the Xunta de Galicia for financial support during their stay at Heinrich-Heine University and acknowledge the Ministerio de Educación y Ciencia (Project CTQ2004-07683-C02-02). S.F., R.K., and C.A.M.S. thank Carl Sandhagen for his efforts to establish the setup for full fluorescence correlation spectroscopy. C.A.M.S. additionally acknowledges the Bundesministerium für Bildung, Forschung und Technologie (BioFuture Grant 0311865).

Supporting Information Available: The derivation of the number of collisions N_{coll} during the lifetime of an encounter complex, and the estimation of the reaction probability P_r during a collision between guest and host. This material is available free of charge via the Internet at http://pubs.acs.org.

JA0508976